Anal. Chem. **2007,** *79,* 3487−3493

Localized Surface Plasmon Coupled Fluorescence Fiber-Optic Biosensor with Gold Nanoparticles

Bao-Yu Hsieh,[†] Ying-Feng Chang,[‡] Ming-Yaw Ng,[§] Wei-Chih Liu,[§] Chao-Hsiung Lin,[||] Hsieh-Ting Wu,[⊥] and Chien Chou*[,†,‡,⊥]

Institute of Biophotonics, Faculty of Life Sciences, and Institute of Biomedical Imaging and Radiological Sciences, National Yang Ming University, Taipei, Taiwan 112, Institute of Optical Sciences, National Central University, Jung-Li, Taiwan 320, and Institute of Physics, National Taiwan Normal University, Taipei, Taiwan 116

A novel fiber-optic biosensor based on a localized surface plasmon coupled fluorescence (LSPCF) system is proposed and developed. This biosensor consists of a biomolecular complex in a sandwich format of <antibody/antigen/Cy5-antibody-gold nanoparticle (GNP)>. It is immobilized on the surface of an optical fiber where a <Cy5-antibody-GNP> complex forms the fluorescence probe and is produced by mixing Cy5-labeled antibody and protein A conjugated gold nanoparticles (Au-PA). The LSPCF is excited by localized surface plasmon on the GNP surface where the evanescent field is applied near the core surface of the optical fiber. At the same time, the fluorescence signal is detected by a photomultiplier tube located beside the unclad optical fiber with high collection efficiency. Experimentally, this novel LSPCF biosensor is able to detect mouse immunoglobulin G (IgG) at a minimum concentration of 1 pg/mL (7 fM) during the biomolecular interaction of the IgG with anti-mouse IgG. The analysis is expanded by a discussion of the amplification of the LSPCF intensity by GNP coupling, and overall, this LSPCF biosensor is confirmed experimentally as a biosensor with very high sensitivity.

During the late 1960s and early 1970s, low-cost optical fibers were used to develop the first chemical sensors. Since then, the evanescent wave fluorescence biosensor has been used in a diverse range of instruments. The importance of the evanescent wave excited fluorescence biosensors is that they show a near-field sensing ability that is able to only detect biomolecules within the interactive region and the system is insensitive to the influence by noninteracting background molecules. Furthermore, the system has a simple optical geometry and can easily be made into a disposable device, which are both also advantages.[1−5] Theoretically, the fiber-optic biosensor is based on total internal reflection at the interface between the unclad fiber core surface and dielectric medium where the refractive indices of fiber core n_{core} and dielectric medium n_{medium} satisfy the condition of $n_{core} > n_{medium}$.[6,7] As a result, the evanescent field decays exponentially into dielectric medium in a perpendicular direction to the interface. The penetration depth d_p is $d_p = \lambda/2\pi n_{medium}[(n_{core}/n_{medium})^2 \sin^2\theta - 1]^{1/2}$, where θ is the incident angle to the interface and λ is the wavelength of laser source. Thus, the evanescent field can only excite fluorescent reporters near the optical fiber surface. As a result, the fluorescence signal created by specific binding to this fiber-optic biosensor is able to separate specific from nonspecific interactions effectively. This results in the fiber-optic biosensor acting as a highly specific and easily manipulated biosensor that can monitor the binding process in real time. However, fiber-optic biosensors have a relatively low detection sensitivity compared to other conventional methods such as enzyme-linked immunosorbent assay and radioimmunoassay.[8−12] As a result of this, fiber-optic biosensors have not been widely used in clinical applications. Currently, development of fiber-optic biosensors has focused primarily on increasing detection sensitivity and specificity during the bioanalysis. Based on the above, therefore, a high sensitive fiber-optic biosensor would be very useful clinically. One major direction that can be followed to enhance detection sensitivity is to focus on integrating the fiber-optic probe with metal nanoparticles (MNPs), which are able to generate localized surface plasma waves on the MNP surface and thus excite fluorescence efficiently. It is because the gold nanoparticle (GNP) shows a strong coupling of the incident laser beam

* To whom the correspondence should be addressed. Tel: 886-2-28267061. Fax: 886-2-28251310. E-mail: cchou@ym.edu.tw.

[†] Institute of Biophotonics, National Yang Ming University.

[‡] National Central University.

[§] National Taiwan Normal University.

[||] Faculty of Life Sciences, National Yang Ming University.

[⊥] Institute of Biomedical Imaging and Radiological Sciences, National Yang Ming University.

(1) Taitt, C. R.; Anderson, G. P.; Ligler, F. S. *Biosens. Bioelectron.* **2005**, *20*, 2470−2487.

(2) Marazuela, M. D.; Moreno-Bondi, M. C. *Anal. Bioanal. Chem.* **2002**, *372*, 664−682.

(3) Mehrvar, M.; Bis, C.; Scharer, J. M.; Moo-Young, M.; Luong, J. H. *Anal. Sci.* **2000**, *16*, 677−692.

(4) Wolfbeis, O. S. *Anal. Chem.* **2002**, *74*, 2663−2678.

(5) Narang, U.; Anderson, G. P.; Ligler, F. S.; Buranst, J. *Biosens. Bioelectron.* **1997**, *12*, 937−945.

(6) Chang, Y. H.; Chang, T. C.; Kao, E. F.; Chou, C. *Biosci. Biotechnol. Biochem.* **1996**, *60*, 1571−1574.

(7) Chan, T. S.; Chou, C.; Han, C. Y.; Wu, H. T.; You, Z. R. In *CLEO/Pacific F2E-(12)-5 Proceedings*, Taipei, Taiwan. 2003; p 734.

(8) Pergande, M.; Jung, K. *Clin. Chem.* **1993**, *39*, 1885−1890.

(9) Benkert, A.; Scheller, F.; Schossler, W.; Hentschel, C.; Micheel, B.; Behrsing, O.; Scharte, G.; Stocklein, W.; Warsinke, A. *Anal. Chem.* **2000**, *72*, 916−921.

(10) Monaci, L.; Tregoat, V.; Hengel, A. J.; Anklam, E. *Eur. Food Res. Technol.* **2006**, *223*, 149−179.

(11) Bellet, D. H.; Wands, J. R.; Isselbacher, K. J.; Bohuon, C. *Proc. Natl. Acad. Sci. U.S.A.* **1984**, *81*, 3869−3873.

(12) Stone, R. T.; Maurer, R. R. *Biol. Reprod.* **1973**, *20*, 947−953.

10.1021/ac0624389 CCC: $37.00
Published on Web 03/23/2007

to the resonantly driven electron plasmon oscillations, which are called localized surface plasmons (LSPs); these exhibit a strong absorption band in the spectrum of visible range.[13−15] Thus, various studies have proposed a colloidal GNP fiber-optic sensor, where GNPs are coated on the surface of a plastic-clad silica optical fiber. The extinction cross section of the self-assembled GNPs on the unclad portion of optical fiber changes with the refractive index of the environment near the GNP surface. Such a system has a limit of detection (LOD) at 40 pg/mL for staphylococcal enterotoxin B (SEB).[15] In a similar system, 9.8×10^{-11} M biotin−streptavidin interaction has also been measured.[16] Recently, MNP-enhanced fluorescence immunoarrays have been developed,[17−19] where the total internal reflection at a silver island-coated surface is arranged such that the surface plasmon coupled emission signal can be excited and detected.[20−22] In addition, it has been shown that GNPs with a self-assembled monolayer suspended in the reaction solution are also able to effectively improve the sensitivity of fluorophore-mediated biosensors.[23] In this study, we propose a GNP-based fiber-optic biosensor that is able to enhance sensitivity of detection based on their ability to support LSP on GNP. Once the fluorophores are conjugated onto the surface of the GNP, which moves into the region of the evanescent field near the interface of the unclad optical fiber, and as a result, fluorophores can be excited simultaneously. Thus, the localized surface plasmon coupled fluorescence (LSPCF) signal is excited and amplified.[24]

In this study, a fiber-optic biosensor based on LSPCF and a sandwich biomolecular complex of <antibody/antigen/fluorophore-labeled-antibody-conjugated-GNP> immobilized to the surface of optical fiber is proposed and then set up. A novel fluorescence probe in which Cy5-labeled antibody is bound to protein A conjugated with GNPs (20 nm in diameter, $\phi = 20$ nm) (Au-PA) is constructed in order to enhance fluorescence signal by means of LSPCF excitation. In this system, therefore, near 40 fluorophores are excited simultaneously by the LSP on surface of each GNP. The fluorescence signal is then detected by the use of a photomultiplier tube (PMT) integrated with an interference filter in order to detect only a narrow band of fluorescence signal, which improves the signal-to-noise ratio (SNR). The PMT is located beside the unclad optical fiber in this setup[6,7] that is able to provide better fluorescence collection efficiency. Thus, this novel fiber-optic biosensor not only shows significantly enhanced fluorescence signal but also has increased specificity because the antigen−antibody interaction is near the field excitation region of the LSPCF and close to the fiber surface. However, a GNP, when placed at an appropriate distance from a fluorophore, can effectively enhance the fluorescence. In contrast, when GNP is placed too close to a fluorophore, the GNP extracts all electrons in the excited state from the fluorophore. The fluorescence quenching effect results. Or, if it is too far from a fluorophore, the LSP field cannot reach the fluorophore and there will be no effect on the resulting fluorescence intensity.[23]

To verify the applicability of this novel LSPCF fiber-optic immunoassay, the sensitivity of detection based on a sandwich biomolecular complex with different fluorescence probes was tested experimentally. The LOD of this novel LSPCF fiber-optic biosensor using mouse immunoglobulin G (IgG) was found to be 1 pg/mL (7 fM) using a fluorescence probe consisting of Cy5-labeled anti-mouse IgG bound to protein A-conjugated GNPs ($\phi = 20$ nm). Experimentally, the detection sensitivity of the developed LSPCF fiber-optic biosensor on IgG and anti-IgG interactions is significantly enhanced. The theory of evanescent wave scattering by a small metallic sphere is considered in Theoretical Calculations on Fluorescence Signal Enhancement Using a LSPCF Fiber-Optic Biosensor in order to understand the mechanism of fluorescence signal enhancement by the LSPCF fiber-optic biosensor using GNPs.

MATERIALS AND METHODS

All reagents including GNP were purchased from Sigma-Aldrich Co. (St. Louis, MO), unless otherwise stated.

Surface Modification of the Poly(methyl methacrylate) (PMMA) Fiber. A PMMA multimode fiber of 1 mm in diameter was used in this experimental system. The refractive indices of the core and cladding are 1.492 and 1.417, respectively. This implies a numerical aperture (NA) of 0.467 for the plastic fiber. Therefore, a microscope objective (20×) of NA = 0.45 was used in order to maximize the coupling efficiency of the power from the laser into the fiber. As a result, the multiple modes of laser beam propagation in optical fiber produced total reflections that were spread evenly over the surface of the fiber core. This is important in order to obtain high excitation efficiency for the LSPCF in this setup. In addition, the penetration depth d_p of the evanescent wave is 153 nm < d_p < 205 nm depending on the incident angle of the laser beam according to simulation results. In this experiment, the plastic fiber was declad along 4.5 cm of its length by immersing the fiber into ethyl acetate, and then the unclad portion of fiber was washed with 2-propanol to clean the optical fiber surface. Because a multimode plastic fiber was used in this fiber-optic biosensor, a uniform field of evanescent wave on the surface of unclad optical fiber was created. Then, the reaction area on the surface of fiber can be calculated to be 1.413 cm^2 in this experiment. The resulting fiber surface was next modified by chemical adsorption.

To immobilize the biological molecules on the surface of PMMA optical fiber tightly, a chemical adsorption method was adopted to immobilize the capture antibody using covalent binding forces, and this procedure followed the protocol described by Henry et al.[25] Covalent bonds have a higher bonding energy, and

(13) Byun, K. M.; Kim, S. J.; Kim, D. *Appl. Opt.* **2006**, *45*, 3382−3389.
(14) Sokolov, K.; Chumanov, G.; Cotton, T. M. *Anal. Chem.* **1998**, *70*, 3898−3905.
(15) Cheng, S. F.; Chau, L. K. *Anal. Chem.* **2003**, *75*, 16−21.
(16) Chau, L. K.; Lin, Y. F.; Cheng, S. F.; Lin, T. J. *Sens. Actuators, B* **2006**, *113*, 100−105.
(17) Gryczynski, Z.; Malicka, J.; Gryczynski, I.; Matveeva, E.; Geddes, C. D.; Aslan, K.; Lakowicz, J. R. *Proc. SPIE* **2004**, *5321*, 275−282.
(18) Matveeva, E.; Gryczynski, Z.; Malicka, J.; Gryczynski, I.; Lakowicz, J. R. *Anal. Biochem.* **2004**, *334*, 303−311.
(19) Matveeva, E.; Gryczynski, Z.; Lakowicz, J. R. *J. Immunol. Methods* **2005**, *302*, 26−35.
(20) Matveeva, E.; Gryczynski, Z.; Gryczynski, I.; Lakowicz, J. R. XXXX **2004,** *286*, 133−140.
(21) Lakowicz, J. R.; Malicka, J.; Gryczynski, I.; Gryczynski, Z. *Biochem. Biophys. Res. Commun.* **2003**, *307*, 435−439.
(22) Matveeva, E.; Gryczynski, Z.; Malicka, J.; Lukomska, J.; Makowiec, S.; Berndt, K. W.; Lakowicz, J. R.; Gryczynski, I. *Anal. Biochem.* **2005**, *344*, 161−167.
(23) Hong, B.; Kang, K. A. *Biosens. Bioelectron.* **2006**, *21*, 1333−1338.
(24) Johansson, P.; Xu, H.; Kâll, M. **2005**.
(25) Henry, A. C.; Tutt, T. J.; Galloway, M.; Davidson, Y. Y.; McWhorter, C. S.; Soper, S. A.; McCarley, R. L. *Anal. Chem.* **2000**, *72*, 5331−5337.

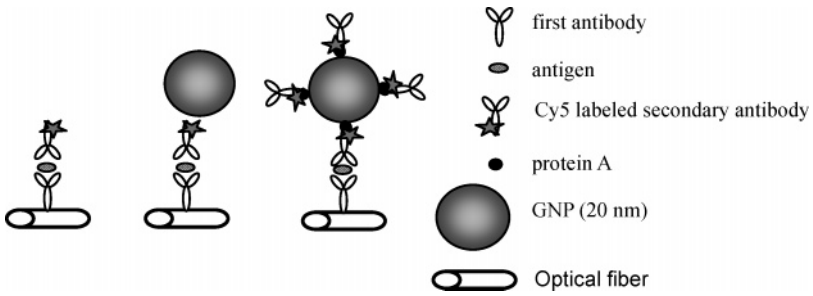

Figure 1. Diagram of the three types of fluorescence probe used in this study.

therefore, the reaction process can tolerate a wider range of pH values in test solutions as well as repeated washing steps. The result is a system that is able to preserve a high surface coverage of the immobilized capture antibody on the fiber surface throughout the experimental procedures. Initially, the PMMA surface is aminated by surface aminolysis with *N*-lithioethylenediamine. This was synthesized by a reaction between ethylenediamine and butyllithium in cyclohexane. Then, the PMMA fiber was soaked in the *N*-lithioethylenediamine solution for 10−15 min. After that, glutaraldehyde, a cross-linking agent, which has two aldehyde groups, was added and allowed to react with chemically modified fibers at room temperature for 1 h. This involved one aldehyde group of glutaraldehyde becoming connected to the NH_2-modified PMMA surface and allowed at a later stage for the other aldehyde group to be connected to either the N-terminal or internal lysine amino groups of a protein molecule such as an antibody.

Biorecognition Molecules and Sandwich Immunoassay. The biosensor was constructed as a sandwiched biomolecular complex consisting of <antibody/antigen/Cy5-antibody-conjugated-GNP>, which was built up on the surface of the optical fiber (Figure 1). Initially, rabbit anti-mouse IgG, the capture biorecognition antibody, was immobilized on the unclad optical fiber surface using the chemical modifications described above. The reaction area of the fiber surface was incubated in the anti-mouse IgG solution at 4 °C overnight. The volume of anti-mouse IgG solution was 8 mL, and its concentration was 10 μg/mL. The surface immobilization of first antibody on the optical fiber was achieved by chemically activating the surface functional groups, which react to any molecules carrying amino groups, i.e., antibodies, antigens, and proteins. To avoid the nonspecific immobilization of antigen or Cy5-labeled antibody during the analysis, which may cause false-positive readout, bovine serum albumin (BSA) proteins were added to quench the surface activation prior to the following incubation of antigen and Cy5-labeled antibody. Therefore, 1 mL BSA was used for 1 h at room temperature, and the concentration of BSA was 10 mg/mL. High-concentration BSA was used in this measurement in order to provide enough BSA to block the area where the capture antibody was not bound. The surplus BSA was washed out in the experiment. Then, different concentrations of mouse IgG solution of 1 mL at 1 ng/mL, 100 pg/mL, 10 pg/mL, 1 pg/mL, and 10 ng/mL nonspecific BSA, respectively, were added into the reaction chamber separately and allowed to interact with the immobilized anti-mouse IgG for 1 h at room temperature to produce different concentrations of the fiber-optic probe. Three different kinds of fluorescence probe consisting of Cy5-labeled anti-mouse IgG with or without conjugated GNP as shown in Figure 1 were made and added to the reaction chamber in separate treatments. Finally, to follow the experimental protocol, the fluorescence signal is then excited and measured by the PMT.[6,7]

Preparation of the Fluorescence Probe. Three kinds of fluorescence probes were tested in this experimental system. They were (1) Cy5-labeled anti-IgG without GNP, (2) Cy5-labeled anti-IgG and GNP (ϕ = 20 nm), which was suspended in PBS solution, and (3) Cy5-labeled anti-IgG bound to Au-PA (ϕ = 20 nm). They are shown in Figure 1. Ten protein A molecules are bound to the surface of each GNP (ϕ = 20 nm).[26] Each protein A molecule contains four Fc terminal binding domains and therefore nearly 40 Cy5 molecules on GNP are excited by the LSP field simultaneously. This arrangement is able to significantly enhance the intensity of fluorescence signal. In order to produce the fluorescence probe 3, Au-PA was mixed with Cy5-labeled anti-mouse IgG and incubated at 4 °C in the dark for 2 h.

To compare the three types of fluorescence probes in terms of their fluorescence signal intensity, the same concentrations of Cy5-labeled anti-mouse IgG and GNP were used in the experiments.

Experimental Setup. The optical setup for the experimental system involves the use of a 658-nm diode laser. In order to achieve the best coupling efficiency of the laser beam to the optical fiber, a 20× microscope objective of NA = 0.45 was used.[6,7] At the same time, a multimode plastic optical fiber (ϕ = 1 mm) was chosen in order to generate multiple modes of laser beam propagation along the fiber, creating a uniform distribution of the evanescent wave on the fiber surface. During the experiments, the laser beam was shone down the fiber such that the condition of NA = 0.45 was satisfied.[27] It is because the surface plasmon peak wavelength of a single gold nanoparticle in water is ~520 nm[28] while in their conjugated forms; although the exactly effective refractive index of the conjugated forms cannot be found, the best guess is the peak wavelength of a conjugated form very similar to the case of a single gold nanoparticle in water since the refractive index of the protein A molecules on the surface of gold nanoparticles is very similar to water. The reason we did not choose the resonance frequency is that the gold nanoparticles also exhibit strong absorption at resonance condition and the fluorescence signals are absorbed possibly by gold nanoparticles when the emission wavelength of fluorescence signals are close

(26) Private communication: Ten or more protein A molecules are bound on each gold nanoparticle (GNP, 20 nm). This information is confirmed by Dr. S. Bagga, a senior technical scientist of Sigma-Aldrich Technical Services Department in Sigma-Aldrich Inc. (St. Louis, MO).
(27) Globe, D. *Appl. Opt.* **1971**, *10*, 2252−2258.
(28) Sugunan, A.; Thanachayanont, C.; Dutta, J.; Hilborn, J. G. *Sci. Technol. Adv. Mater.* **2005**, *6*, 335−340.

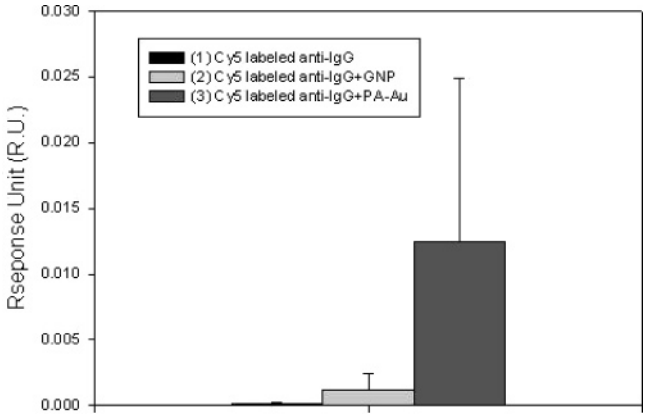

Figure 2. Fluorescence intensities of different fluorescence probes. Analyte, 10 ng/mL IgG. Error bars represent ±1 SD.

to the surface plasmon peak wavelength. In order to avoid the resonance wavelength of gold nanoparticles, incident light with a wavelength of 650 nm was used in the experiments to obtain the fluorescence signals with an emission wavelength of 680 nm. Then, in order to separate the pumping beam (650 nm) from the fluorescence signal, a narrow band interference filter centered at a frequency of 680.4 nm and with a bandwidth of 11.1 nm was attached in front of the PMT in order to obtain a high SNR for the fluorescence signal. During the measurements, a lock-in amplifier was used to detect the fluorescence signal at 800 Hz by intensity modulation. Moreover, the effect of laser intensity fluctuation was reduced by the use of a reference photodetector to monitor laser intensity fluctuation in real time. LabVIEW software was employed for data acquisition during all experiments.

RESULTS

Enhanced Novel Fluorescence Probe. The three different fluorescence probes as shown in Figure 1 were investigated under the same conditions with respect to the concentration of Cy5-labeled anti-IgG and GNPs. In Figure 2, (1) shows the fluorescence intensity response of a conventional fluorescence probe without GNP. This contrasts with (2), where a fluorescence probe coupled with a pure GNP ($\phi = 20$ nm) suspension is shown and there is a 12-fold amplification compared to the conventional fluorescence probe. However, (3) when a fluorescence probe is used made with Cy5-labeled anti-IgG bound to protein A-conjugated GNPs, there is a 245-fold increase in the signal compared to the conventional fluorescence probe. Thus, the ratio of the fluorescence intensities versus the three different fluorescence probes in this analysis is 1:12:245, which is normalized by the fluorescence intensity generated by the conventional fluorescence probe. This agrees with theoretical calculations that are outlined in Theoretical Calculations on Fluorescence Signal Enhancement Using a LSPCF Fiber-Optic Biosensor. In this experiment, to compare three types of fluorescence probe in terms of their fluorescence signal intensity, the same concentration of mouse IgG was 10 ng/mL, while the volume concentrations of Cy5-labeled antibody and GNP are 1 μg/mL and 1.25×10^9 particles/mL, respectively.

Figure 3a shows the temporal responses for the binding of mouse IgG at concentrations of 0, 1, 10, and 100 pg/mL and 1 ng/mL when interacting with the Cy5-labeled anti-mouse IgG, which was bound to the Au-PA; this analysis was carried out at

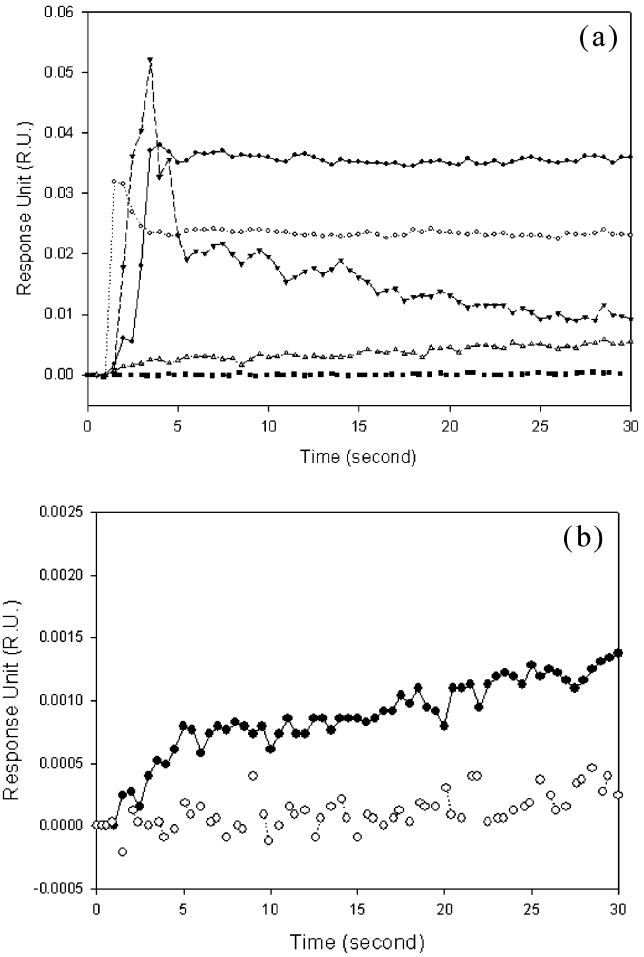

Figure 3. (a) Analysis if the binding process of the Cy5-labeled anti-mouse IgG to protein A-conjugated GNP with different concentrations of mouse IgG. Key: ●, 1 ng/mL; ○, 100 pg/mL; ▼, 10 pg/mL; △, 1 pg/mL; ■, 10 ng/mL nonspecific BSA]. (b) Nonspecific BSA binding test. Key: ○, 10 ng/mL nonspecific BSA; ●, 1 pg/mL IgG.

fixed concentrations of Cy5-labeled anti-mouse IgG and GNP. Under these conditions, the fluorescence signals increased rapidly immediately after the addition of the fluorescence probe and increased until equilibrium was reached as shown Figure 3a. In this experiment, the nonspecific binding by use of 10 ng/mL BSA to present zero concentration of mouse IgG was arranged and measured in Figure 3b. It shows the difference in the measurement between the concentration of 0 and 1 pg/mL mouse IgG that verifies the sensitivity of fluorescence probe 3 apparently. This implies that the LOD of this novel fiber-optic biosensor is 1 pg/mL (7 fM) when using the GNP-induced LSPCF enhancement. In contrast to this, the LOD was 100 ng/mL for the conventional fluorescence probe using Cy5-labeled anti-mouse IgG without GNP as shown in Figure 4. Thus, there was a 10^5-fold enhancement in detection sensitivity for this novel LSPCF fiber-optic biosensor compared to the conventional fluorescence probe. A linear relationship between the fluorescent intensity (response unit, RU) and the log of the IgG concentration over the range from 0 pg/mL to 1 ng/mL can be seen in Figure 5, where the correlation is $R^2 = 0.9042$. A similar relationship between the fluorescence signal and a log scale of SEB at low concentrations was demonstrated by using a fiber-optic biosensor.[16] The RU is defined as the

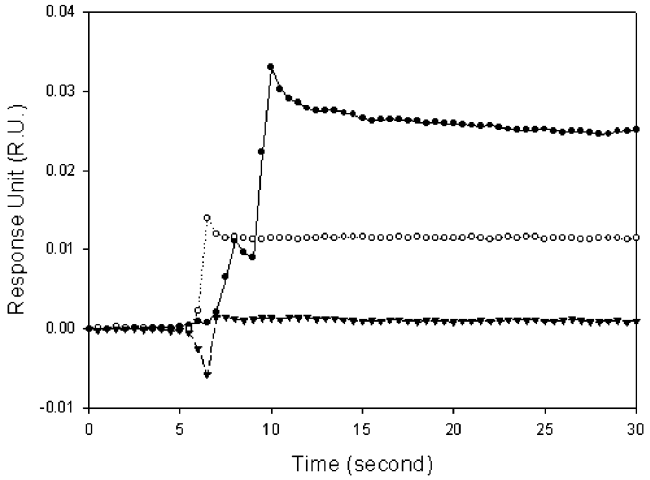

Figure 4. Binding kinetics of Cy5-labeled anti-mouse IgG to mouse IgG at different concentrations: ●, 1000 ng/mL; ○, 500 ng/mL; ▼, 100 ng/mL.

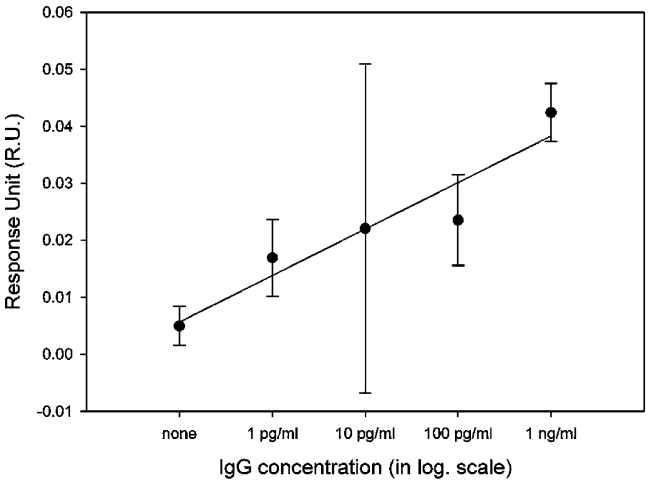

Figure 5. Linear regression of the mouse IgG concentration dependence. (R^2 = 0.9042).

fluorescence signal saturation level subtracted from the background level.

Theoretical Calculations on Fluorescence Signal Enhancement Using a LSPCF Fiber-Optic Biosensor. The fluorescence signal enhancement with a LSPCF fiber-optic biosensor is associated with the local-field enhancement from the GNPs and is due to surface plasmon excitation. To calculate fluorescence signal enhancement, the near-field intensity of the local-field enhancement in the vicinity of the GNPs by the illuminating evanescent waves is now considered theoretically. The scattering of the evanescent waves by a GNP is shown in Figure 6. The core of a multimode optical fiber can be approximated to a dielectric plane medium, and the fiber and surrounding medium can be separated by a plane interface ($y-z$ plane). The GNP, as a metallic sphere with radius r, is placed at a distance d above the interface. Evanescent waves from the surface of the bare core are coupled with the LSP of the GNP when total internal reflection of the plane waves propagating in the fiber occurs. The theory for the scattering of the evanescent waves by a small dielectric sphere was studied by Chew et al. in 1979.[29] The total cross section for

(29) Chew, H.; Wang, D. S.; Kerker, M. *Appl. Opt.* **1979**, *18*, 2679−2687.

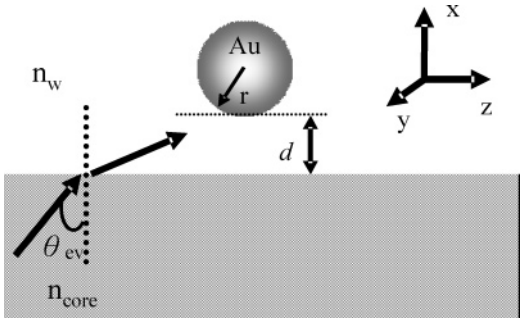

Figure 6. Scattering of evanescent waves by a GNP. The refractive indices of the core of a fiber (n_{core}) and of the medium around the GNP (n_w) are 1.492 and 1.33, respectively. The refraction index of the GNP is 0.166 + 3.15i at λ = 650 nm. The GNP is placed at a distance d above the surface of the step-index multimode fiber.

extinction and scattering of the evanescent waves by a small metallic particle was derived by Quinten et al.,[30] and the multiple scattering between the sphere and the plane interface is ignored. In this paper, the small metal particle is far from the dielectric interface ($d > 2r$) because the size of IgG and anti-IgG is 6.5 ± 0.9 nm according to AFM tapping mode image.[31] Therefore, the sandwich immunocomplex height can be calculated to be ~20 nm. Addition to protein A and chemical adsorption, $d > 2r$ can be assumed. Because the small metal particle is far from the optical fiber ($d > 2r$), the scattering theory for the evanescent waves satisfies first-order approximation when calculating the field intensity in the vicinity of a GNP. The scattered electric field of a GNP with p- or s-polarization is expressed by

$$\vec{E}_{sca}^{s,p} = \sum_{n=1}^{\infty}\sum_{m=-n}^{n} \frac{i}{n_w^2 k_w} a_n \alpha_{TM}^{s,p}(n,m)\left[\nabla \times h_n^{(1)}(\rho)\vec{X}_{nm}\right] + b_n \alpha_{TE}^{s,p}(n,m)\left[h_n^{(1)}(\rho)\vec{X}_{nm}\right] \quad (1)$$

Where a_n and b_n are the Mie coefficients and the functions $\alpha_{TM}^{s,p}$ and $\alpha_{TE}^{s,p}$ are expansion coefficients. k_w is the wave number of the electromagnetic wave propagating in water, and $\rho = k_w r$. $h_n^{(1)}$ is the first-order spherical Hankel function, and $\vec{X}_{nm}$ is the vector spherical harmonics function.[30]

The incident light propagates in a multimode fiber with various propagation constants β (=sin θ_{inc}), and the range of β is from 0.0 to 0.45. Figure 7b shows the decay length of the evanescent waves when the incident light propagates in the step-index multimode fiber with different propagation constants β at λ = 650 nm. The NA of the incident focusing laser beam is 0.45. The section of the unclad optical fiber is shown in Figure 7a. The decay length of the evanescent waves will increase with a larger β, and the range of the decay lengths will be 153−205 nm. When the GNP is illuminated by evanescent waves, the averaged scattered electric field in the vicinity of the GNP is,

$$\left\langle \vec{E}_{scat}^{p} \right\rangle = \frac{1}{0.45}\int_0^{0.45} \vec{E}_{scat}^{p}(\beta)\, d\beta \quad (2)$$

Only p-polarization scattered electric fields are considered in the

(30) Quinten, M.; Pack, A.; Wannemacher, R. *Appl. Phys. B* **1999**, *68*, 87−92.
(31) Lee, K. B.; Park, S. J.; Mirkin, C. A.; Smith, J. C.; Mrksich, M. *Science* **2002**, *295*, 1702−1705.

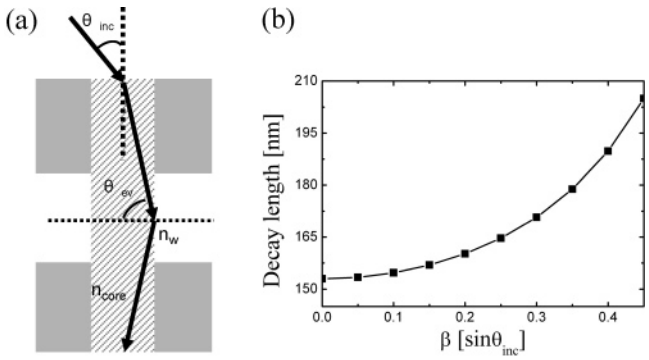

Figure 7. (a) Section of an uncladded fiber. (b) Decay length of the evanescent wave as a function of β at $\lambda = 650$ nm. Indices of refraction of the core of the fiber and surrounding medium (water) are 1.492 and 1.33, respectively. The range of the decay length is from 153 to 205 nm.

calculation since the near-field intensity of the s-polarization field of GNP is much weaker than that of the p-polarization field.[33] Since the fluorescence signal from the lower half of a GNP surface is screened by GNP itself, only the fluorescence intensity excited on the upper half surface of GNP is considered. Then the intensity ratio of the averaged fluorescence intensity with a GNP $\langle I_{ev}\rangle$ to that of the averaged intensity by evanescent wave without GNP $\langle I_0\rangle$ is expressed by

$$\frac{\langle I_{ev}\rangle}{\langle I_0\rangle} = \frac{\int_{-(\pi/2)}^{(\pi/2)} \int_0^{\pi} |\langle \vec{E}^{p}_{scat}\rangle + \langle \vec{E}^{p}_{inc}\rangle|^2 \sin\theta d\theta d\phi}{|\langle \vec{E}^{p}_{inc}\rangle|^2} \qquad (3)$$

$\langle I_0\rangle$ is measured at a distance d above the surface of the optical fiber.

According to our calculations, the averaged fluorescence intensity near a GNP is enhanced to eight times compared with the intensity without GNP. Compared with the experimental results, the magnification of the near-field intensity of GNP is on the same order of magnitude as the increase in fluorescence intensity from the GNP suspension. It should be noticed that a realistic GNP is not a perfect sphere and the near-field intensity of a realistic GNP will generally be stronger than that of a GNP with a perfect spherical shape. Therefore, our theoretical results seem to be slightly weaker than the experimental measurements presented under Enhanced Novel Fluorescence Probe. If a situation with multiple fluorophores attached to each GNP is considered, the fluorescence signal is proportional to the number of fluorophores. It is estimated that there are 20 or more Cy5 on the upper half of a GNP in this experiment. The predicted enhanced ratio of the fluorescence signal thus becomes 160 or so. Therefore, the ratio of intensities of three different fluorescence probes by theoretical calculations is 1:8:160, and this ratio agrees well with the experimental measurements in Enhanced Novel Fluorescence Probe.

DISCUSSION AND CONCLUSIONS

A LSPCF fiber-optic biosensor that features an integrated optical fiber evanescent wave sensor with GNPs that use a sandwich structure <antibody/antigen/Cy5-labeled-antibody-protein-A-conjugated-GNP> system is demonstrated. Mouse IgG antigen is experimentally detected at a best sensitivity of 1 pg/mL. There are two effects involved in this novel biosensor; the first is the LSP excited by the evanescent wave on the GNPs and this produces a strong local electromagnetic field within 50−60 nm around the GNP surface to efficiently enhance the fluorescence signal.[15] This is more localized than a planar surface plasmon effect and is able to improve local specificity of antigen−antibody interaction. In the meantime, the nonspecific binding can be ignored because a very low concentration of nonspecific antigen exists in the region of LSP field. Figure 3b shows the nonspecific background signal at zero concentration of mouse IgG that verifies the prediction. Second, there are multiple fluorophores labeled antibody coated onto the GNPs by using conjugation with protein A as linkers to the surface, and this allows nearly 40 Cy5 molecules on each GNP surface being simultaneously excited in this measurement. These two effects synergistically multiply together and produce a significant improvement in the sensitivity of the system compared to a conventional fluorescence probe.

In addition, protein A has the ability to selectively bind the Fc terminals of IgG to provide orientation when connecting the immune complex.[32] Protein A thus not only plays a role as a linker to the recording antibody on the GNP but also provides an appropriate distance between GNP and the fluorophores to avoid fluorescence quenching effect. According to Hong and Kang[23] and Borejdo et al.,[33] the fluorescence quenching happened within ~5 nm distance from the surface of GNP in this experiment. Therefore, an appropriate distance between GNP and the fluorophore is important so that GNP can more effectively enhance the fluorescence and prevent fluorescence quenching at the same time.[17,23] This is an important feature of this LSPCF biosensor when monitoring the binding kinetics of biomolecular interactions at low concentrations.

However, the LSPR is strongly dependent on the nanoparticle size, shape, interparticle spacing, and local dielectric environment.[34,35] Thus, to optimize the conditions for this novel fiber-optic biosensor to give highly efficient LSPCF excitation becomes important to the development of a biosensor. This is particularly true when monitoring the binding kinetics of very low abundance protein−protein interaction in real time, and further research is being carried out on this at the present time.

In GNP, the polarization charge oscillations can be excited by visible light. The absorption efficiency of GNP with a diameter of 20 nm shows that the surface plasmon peak wavelength in water is ~520 nm.[28] The reason we did not choose the resonance frequency is that the GNPs also exhibit strong absorption at resonance condition and the fluorescence signals are absorbed possibly by GNPs when the emission wavelength of fluorescence signals are close to the surface plasmon peak wavelength. In order to avoid the resonance wavelength of GNPs, incident light with a wavelength of 650 nm was used in the experiments to obtain the fluorescence signals with an emission wavelength of 680 nm. Generally, local-field enhancement around GNP at 650 nm is weaker than that at 520 nm; however, the averaged fluorescence

(32) Anderson, G. P.; Jacoby, M. A.; Ligler, F. S.; King, K. D. *Biosens. Bioelectron.* **1997**, *12*, 329−336.
(33) Borejdo, J.; Gryczynski, Z.; Calander, N.; Muthu, P.; Gryczynski, I. *Biophys. J.* **2006**, *91*, 2626−2635.
(34) Haes, A. J.; Zou, S.; Schatz, G. C.; Van Duyne, R. P. *J. Phys. Chem. B* **2004**, *108*, 109−116.
(35) Haes, A. J.; Zou, S.; Schatz, G. C.; Van Duyne, R. P. *J. Phys. Chem. B* **2004**, *108*, 6961−6968.

intensity by GNP at 680 nm still can be enhanced to ~8 times the fluorescence intensity without GNP. There is strong enhancement due to the surface plasmon in this arrangement.

We have verified experimentally that the best sensitivity of LSPCF fiber-optic biosensor was 1 pg/mL when detecting mouse IgG interacting with anti-mouse IgG. In the meantime, the linear dynamic range of this novel biosensor from background to 1 ng/mL on mouse IgG detection was achieved experimentally. Finally, the theoretical calculations on fluorescence signal enhancement by LSPCF excitation are calculated and are consistent with our experimental results. With proper arrangement of this novel fluorescence probe, the LSPCF fiber-optic biosensor shows great potential in biomolecule interaction studies at very low concentrations in a clinical environment.

ACKNOWLEDGMENT

This research is partially supported by National Science Council of Taiwan, through Grant NSC 94-2215-E-010-001.

Received for review December 26, 2006. Accepted February 16, 2007.

AC0624389